Calculation of Vibrational Infrared Intensities and Raman Activities Using Explicit Anharmonic Wave Functions†

Peter Seidler,* Jacob Kongsted,‡ and Ove Christiansen§

The Lundbeck Foundation Center for Theoretical Chemistry, Department of Chemistry, University of Aarhus, Langelandsgade 140, DK-8000 Aarhus C, Denmark

Received: January 15, 2007; In Final Form: March 16, 2007

Methods for automatic computation of IR intensities and Raman activities are described using vibrational self-consistent field (VSCF) and vibrational configuration interaction (VCI) wave functions. Inclusion of effects due to anharmonicity in the potential energy and property surfaces are found to improve the results substantially as compared to experimental data. Sample calculations employing water and formaldehyde are presented, allowing for comparison between different vibrational methods. The convergence with respect to excitation level in VCI and the extent of mode coupling in the potential and property expansions is investigated. In addition, different electronic methods used for generating the potential and property surfaces, namely CCSD, CCSD(T), DFT/B3LYP, and DFT/CAM-B3LYP have been compared. Details of the potential and property surfaces may have significant effects on the IR and Raman intensities.

I. Introduction

In vibrational spectroscopy, including both IR and Raman, the transition energies as well as the transition probabilities provide spectroscopic fingerprints and information about the internal motions of molecular systems. Determination of IR intensities and Raman activities by ab initio methods requires the calculation of transition matrix elements of the dipole moment and polarizability tensor operators, respectively, between the initial and final states. A common starting point for most ab initio methods is the Born−Oppenheimer approximation in which the electronic and nuclear degrees of freedom are separated so that the nuclear motion is determined by a potential given by the electronic energy. The total wave function is then a product of a nuclear and an electronic function. At present there are well-established electronic structure methods, e.g., configuration interaction (CI), coupled cluster (CC), and density functional theory (DFT) enabling quite accurate calculations of the electronic part of the transition matrix elements as a function of the nuclear coordinates. However, the electronic calculation is only one part of the problem, the other being the inclusion of the vibrational motion to obtain the final matrix element. Presently, the double harmonic approximation seems to be the most common solution to this problem. In this simple approximation the nuclear potential is assumed to be purely harmonic and the properties, i.e., the dipole moment or the polarizability, are expanded to first order in the nuclear coordinates. This allows for an easy calculation of the total transition matrix elements using the algebra of the quantum mechanical harmonic oscillator.

The potential and property surfaces are anharmonic by nature and as electronic structure methods become increasingly accurate a large part of the discrepancies with experiment can be ascribed to the simplicity of the double harmonic approximation. Thus, just as it is now possible to address the electron correlation problem systematically using hierarchies of *N*-electron models and correlation consistent basis sets,[1] it is desirable to develop automated methods for the calculation of energies and (transition) properties beyond the harmonic approximation. Several methods have been proposed for a more accurate description of the vibrational motion. One standard approach is to treat anharmonicity using perturbation theory[2] where effects beyond the harmonic Hamiltonian is treated as a perturbation. This allows also for calculation of IR intensities for fundamental vibrations, see ref 3 for a discussion. Another branch of methods is based on the vibrational self-consistent field (VSCF)[4,5] including vibrational Møller−Plesset (VMP) perturbation theory,[6,7] vibrational configuration interaction (VCI),[8−11] and vibrational coupled cluster (VCC).[10,12] A common feature of all these methods is their dependence on accurate potential energy as well as property surfaces. Obtaining these surfaces from electronic structure calculations is an important research area; see, e.g., refs 12 and 13 and references therein. A completely different approach is the Car−Parrinello molecular dynamics[22] (CPMD) method in which the potential is generated on the fly and spectra are calculated on the basis of the autocorrelation function from a classical simulation, including potentially also quantum corrections.[23] This method, however, is generally aimed at extended systems and based on DFT. For high accuracy the time-independent methods discussed above are therefore preferred. In addition, the ability to obtain the potential and property surfaces using a variety of electronic structure methods provides a good basis for comparing these methods.

The present work focuses on the calculation of IR intensities and Raman activities of water and formaldehyde using the variational VSCF and VCI methods. We use response theoretical methods for calculation of transition properties and energies, circumventing the problems of nonorthogonal states in VSCF. Calculations of IR intensities of water and formaldehyde using VCI with DFT as the electronic structure method has been reported earlier by Burcl. et al.[24] Another example is the work

† Part of the "Thom H. Dunning, Jr., Festschrift".

* To whom correspondence should be addressed. E-mail: seidler@chem.au.dk.

‡ E-mail: kongsted@chem.au.dk.

§ E-mail: ove@chem.au.dk.

10.1021/jp070327n CCC: $37.00
Published on Web 05/03/2007

of Oyanagi et al.[25] reporting VCI and IR calculations on methane using a combination of CCSD(T) and MP2 electronic structure methods. To the best of our knowledge vibrational Raman activities for polyatomic molecules have only been calculated within the double harmonic approximation; see, e.g., refs 26−28. For diatomic molecules, activities have been obtained by numerical solution of the nuclear Schrödinger equation; see ref 29.

It should be noted that neither VSCF nor VCI are restricted to four-atomic molecules but can be applied to larger systems as well. However, the increase in cost of a VCI calculation with the size of the system is significant, and the search for alternative approaches is a topic of ongoing research; see, e.g., refs 6, 7, 10, and 30. The generation of potential and property surfaces for larger systems is also very time-consuming and another important research topic.

In addition to comparing the results with results obtained using the double harmonic approximation the convergence of VCI is examined. Also the electronic calculations have been carried out using a variety of methods, i.e., CCSD, CCSD(T), DFT/B3LYP, and DFT/CAM-B3LYP.[31] This allows for a comparison of the ability of these methods to provide the necessary accuracy in the electronic structure calculations.

The absorption spectrum of water due to vibrational motion is important in many contexts and has been intensively studied. Specialized treatments are possible for water having only 3 nuclei and 10 electrons, and high accuracy calculations of the vibrational energies of gas-phase water have been reported in many previous studies.[32,33] In the case of liquid water classical molecular dynamics[34] as well as CPMD[22,33] have been used to obtain IR and Raman spectra.

The vibrations of formaldehyde have also previously been considered in many high accuracy studies.[24,36−41] Our emphasis here is to illustrate and test our new methods for calculating vibrational transition properties in combination with different electronic structure methods. We shall not enter into a detailed discussion of all the past calculations of vibrational energies, and only refer to the above references as entries to this literature.

In section II, we give a review of the necessary theory of IR and Raman spectroscopy as well as of vibrational structure theory. Section III describes the computational details and the results are discussed in section IV. Section V contains a summary and outlook.

II. Theory

We first briefly expose, in subsection IIA and IIB, the basic theory behind vibrational IR and Raman spectroscopy to define what quantities are to be calculated and the underlying assumptions. We use semiclassical theories for the interaction between light and matter, i.e., a classical treatment of the electromagnetic field and a quantum mechanical treatment of the molecules. Similar theories involving quantized radiation fields can be found in refs 42 and 43. In section IIC we discuss how to calculate the relevant quantities from vibrational structure theory and electronic structure theory in combination.

A. IR Intensities. Using first-order perturbation theory one arrives at the result that the transition rate related to one-photon absorption is proportional to $|\langle \mathrm{f}|H'|\mathrm{i}\rangle|^2$. Here $|\mathrm{f}\rangle$ and $|\mathrm{i}\rangle$ are the final and initial states respectively and H' is an operator describing the interaction with the electromagnetic field. Invoking the dipole approximation, the perturbation operator can be written explicitly as $H' = -\boldsymbol{\mu}\cdot\mathbf{E}$, $\mathbf{E}$ being the electric field and $\boldsymbol{\mu}$ the electric dipole operator.

Assuming the Born−Oppenheimer approximation is valid, the total wave function can be written as a product of a nuclear and an electronic part. The nuclear part describes both the rotation and vibration of the molecule. In the next approximation we neglect the coupling between vibration and rotation and discard the rotational part of the nuclear wave function in favor of a classical rotational averaging assuming a large ensemble of molecules at hand. With these approximations the quantity to be calculated is

$$\frac{1}{3}|\langle \mathrm{v_f}|\langle \mathrm{e_g}|\boldsymbol{\mu}|\mathrm{e_g}\rangle|\mathrm{v}_i\rangle|^2\cdot|\mathbf{E}|^2 = \frac{1}{3}|\langle \mathrm{v_f}|\boldsymbol{\mu}(\mathbf{Q})|\mathrm{v_i}\rangle|^2\cdot|\mathbf{E}|^2 \qquad (1)$$

where $|\mathrm{v_f}\rangle$ and $|\mathrm{v_i}\rangle$ are the final and initial vibrational states, $|\mathrm{e_g}\rangle$ is the electronic ground state, and $\boldsymbol{\mu}(\mathbf{Q}) = \langle \mathrm{e_g}|\boldsymbol{\mu}|\mathrm{e_g}\rangle$ is the dipole moment as a function of the nuclear coordinates, $\mathbf{Q}$.

A standard procedure is to invoke the double harmonic approximation where the vibrational states are simply assumed to be harmonic oscillator states expressed in the normal coordinates of the molecule. When $\boldsymbol{\mu}(\mathbf{Q})$ is expanded to first order in each normal coordinate, simple expressions for the transition matrix elements are obtained. Such expressions are widely used, in particular in ab initio methods where the IR intensities in this way can be calculated on the basis of analytical calculation of the dipole gradients.

Instead of this simple approach the VSCF and VCI methods open for the possibility of using the full potential energy and dipole surfaces giving more accurate results. Especially, the double harmonic approximation only supplies nonzero matrix elements for the fundamental transitions. Using explicit vibrational wave functions allows for the calculation of finite transition matrix elements for all states included in the calculation in addition to providing more accurate transition properties for the fundamentals. The problem of representing the potential and property surfaces while at the same time restricting the number of needed electronic structure calculations is, however, not a trivial task. This will be discussed briefly below.

The calculated transition intensities are reported in km/mol using the expression for the integrated absorption coefficient,

$$A(\nu) = \frac{N_A}{6c^2\epsilon_0\hbar^2}E_{\mathrm{fi}}|\langle \mathrm{v_f}|\boldsymbol{\mu}(\mathbf{Q})|\mathrm{v_i}\rangle|^2(n_\mathrm{i} - n_\mathrm{f}) \qquad (2)$$

Here c is the speed of light, ϵ_0 the permittivity of vacuum, and E_{fi} the energy difference between the final and initial states. The factor $(n_\mathrm{i} - n_\mathrm{f})$ is the difference in the fraction of molecules in the initial and final states and thus depends on temperature. All results in this work are obtained by setting this factor equal to one corresponding to zero temperature. This is a good approximation because n_f for the molecules studied in this work is negligible according to the Boltzmann distribution. For molecules with low-frequency modes, however, it may be important to include temperature effects directly.

B. Raman Scattering. As in the section on IR theory, we suppose that the dipole approximation is valid. In Raman spectroscopy the transitions between states are caused by an induced dipole moment

$$\boldsymbol{\mu}_{\mathrm{ind}} = \boldsymbol{\alpha}\cdot\mathbf{E} \qquad (3)$$

where α is the polarizability tensor.

Suppose the electric field is described in complex form as

$$\mathbf{E} = \frac{1}{2}(\tilde{\mathbf{E}}_0 e^{-i\omega t} + \tilde{\mathbf{E}}^*_0 e^{i\omega t}) \quad (4)$$

From perturbation theory one obtains an expression for the induced transition dipole moment. The first-order terms corresponding to Raman scattering are given as[44]

$$(\mu_\rho^{(1)})_{fi} = \frac{1}{2\hbar}\sum_\sigma \sum_r \left(\frac{\mu_{fr,\rho}\mu_{ri,\sigma}}{\omega_{ri} - \omega} + \frac{\mu_{fr,\sigma}\mu_{ri,\rho}}{\omega_{rf} + \omega}\right)\tilde{E}_{0,\sigma} e^{-i(\omega-\omega_{fi})t} + cc \quad (5)$$

where $\boldsymbol{\mu}_{fi} = \langle f|\boldsymbol{\mu}|i\rangle$, and σ and ρ specify general components of the vectors. The summation over r includes all states $|r\rangle$ in the system. The general transition polarizability tensor is now defined as

$$(\alpha_{\rho\sigma})_{fi} = \frac{1}{\hbar}\sum_r \left(\frac{\mu_{fr,\rho}\mu_{ri,\sigma}}{\omega_{ri} - \omega} + \frac{\mu_{fr,\sigma}\mu_{ri,\rho}}{\omega_{rf} + \omega}\right) \quad (6)$$

Once we have calculated this quantity, we know the amplitude of the induced dipole moment. The classical expression for the field of an oscillating dipole can then be used to calculate the intensity of the scattered light.

To get a tractable expression, we invoke the Born−Oppenheimer approximation. As in the case of IR spectroscopy, we ignore rotation in favor of a classical isotropic averaging. The rotational contributions to ω_{ri} and ω_{rf} in the denominators of eq 6 are small and can be ignored as long as only vibrational spectroscopy is considered. All calculations can thus be done in the molecule-fixed coordinate system; that is, we need to calculate

$$\hat{\alpha}_{\rho\sigma} = \frac{1}{\hbar}\sum_{e_r,v_r}\left(\frac{\langle v_f|\langle e_f|\hat{\mu}_\rho|e_r\rangle|v_r\rangle\langle v_r|\langle e_r|\hat{\mu}_\sigma|e_i\rangle|v_i\rangle}{\omega_{e_re_f} + \omega_{v_rv_f} - \omega} + \frac{\langle v_f|\langle e_f|\hat{\mu}_\sigma|e_r\rangle|v_r\rangle\langle v_r|\langle e_r|\hat{\mu}_\rho|e_i\rangle|v_i\rangle}{\omega_{e_re_f} + \omega_{v_rv_f} + \omega}\right) \quad (7)$$

Next we use a set of approximations originally due to Placzek.[44,45] Because we consider only vibrational spectroscopy, the initial and final electronic states are both equal to the electronic ground state, $|e_g\rangle$. Furthermore, the summation in eq 7 can be split in two parts, one containing a summation over vibrational states with the intermediate electronic state being the ground state and one containing the remaining terms,

$$\hat{\alpha}_{\rho\sigma} = \frac{1}{\hbar}\sum_{v_r}\left(\frac{\langle v_f|\langle e_g|\hat{\mu}_\rho|e_g\rangle|v_r\rangle\langle v_r|\langle e_g|\hat{\mu}_\sigma|e_g\rangle|v_i\rangle}{\omega_{v_rv_f} - \omega} + \frac{\langle v_f|\langle e_g|\hat{\mu}_\sigma|e_g\rangle|v_r\rangle\langle v_r|\langle e_g|\hat{\mu}_\rho|e_g\rangle|v_i\rangle}{\omega_{v_rv_f} + \omega}\right) + \frac{1}{\hbar}\sum_{e_r\neq e_g}\left(\frac{\langle v_f|\langle e_g|\hat{\mu}_\rho|e_r\rangle\langle e_r|\hat{\mu}_\sigma|e_g\rangle|v_i\rangle}{\omega_{e_re_g} - \omega} + \frac{\langle v_f|\langle e_g|\hat{\mu}_\sigma|e_r\rangle\langle e_r|\hat{\mu}_\rho|e_g\rangle|v_i\rangle}{\omega_{e_re_g} + \omega}\right) \quad (8)$$

In the last sum we have assumed that $|\omega_{e_re_g} \pm \omega| \gg \omega_{v_rv_i}$ or $\omega_{v_rv_f}$. With this assumption the vibrational energy differences can be ignored and closure over vibrational states have been used to remove the sum over v_r.

From the first sum, denoted the ionic part of the vibrational transition polarizability, we see that in the case of non-resonant spectroscopy, the denominators will be large and the terms can be ignored. This leaves us with only the terms in the second sum. We now define the electronic part of these terms as the standard adiabatic dynamic polarizability tensor,

$$\alpha_{\rho\sigma}^{e_r\neq e_g}(\mathbf{Q}) = \frac{1}{\hbar}\sum_{e_r\neq e_g}\left(\frac{\langle e_f|\hat{\mu}_\rho|e_r\rangle\langle e_r|\hat{\mu}_\sigma|e_i\rangle}{\omega_{e_re_f} - \omega} + \frac{\langle e_f|\hat{\mu}_\sigma|e_r\rangle\langle e_r|\hat{\mu}_\rho|e_i\rangle}{\omega_{e_re_f} + \omega}\right) \quad (9)$$

This quantity can be obtained using standard electronic structure theoretical methods. The challenge is now to calculate the vibrational transition matrix element of this quantity, including anharmonic effects in both the potential and property surfaces, giving the final transition polarizability,

$$(\alpha_{\rho\sigma}^{e_r\neq e_g})_{v_f,v_i} = \langle v_f|\alpha_{\rho\sigma}(\mathbf{Q})|v_i\rangle \quad (10)$$

In actual experiments the irradiation/observation geometry is an important factor.[44] In this paper the geometry independent Raman activity,

$$S = \frac{2\omega_{fi}}{\hbar}(45a^2 + 7\gamma^2) \quad (11)$$

and the depolarization ratio,

$$\rho = \frac{3\gamma^2}{45a^2 + 4\gamma^2} \quad (12)$$

are reported where a and γ are the tensor invariants

$$a = \frac{1}{3}(\alpha_{xx} + \alpha_{yy} + \alpha_{zz}) \quad (13)$$

$$\gamma^2 = \frac{1}{2}(|\alpha_{xx} - \alpha_{yy}|^2 + |\alpha_{yy} - \alpha_{zz}|^2 + |\alpha_{zz} - \alpha_{xx}|^2) + 3(|\alpha_{xy}|^2 + |\alpha_{yz}|^2 + |\alpha_{yz}|^2) \quad (14)$$

These expressions can be used together with other parameters such as the irradiance and temperature to give the scattering intensity in a concrete setup.[44] In addition it should be noted that the calculated activities correspond to the Stokes lines of a spectrum because we always assume the initial vibrational state to be the ground state.

C. Vibrational Structure Theory. The theory of VSCF is well-known in vibrational theory.[4,5] In VSCF the wave function is described by a direct product of one-mode functions. These one-mode functions are variationally and self-consistently optimized using a basis of functions, usually denoted modals, specific to each mode. In addition to providing results on its own, the VSCF method is also used to provide optimized modals for use by correlated methods.

VCI is the simplest way to include correlation between the vibrational modes. The wave function is simply expanded in Hartree products based on the optimized modal basis generated by the VSCF calculations,

$$|\mathrm{VCI}\rangle = |\Phi_{ref}\rangle + \sum_\mu C_\mu \tau_\mu |\Phi_{ref}\rangle \quad (15)$$

and the Schrödinger equation is solved in this particular basis. Here $|\Phi_{ref}\rangle$ is the VSCF reference state and C_μ are the coefficients of the vectors $\tau_\mu|\Phi_{ref}\rangle$ in the excitation space. In this notation τ_μ is an operator that promotes modals from occupied levels in the reference state to unoccupied levels. This can be given an exact formulation in second quantization[12] but

TABLE 1: Comparison with Experimental IR Line Positions and Intensities for H_2O[a]

	Exp[b]		CCSD(T) d-aug-cc-pVTZ						CCSD d-aug-cc-pVTZ		B3LYP aug-cc-pVTZ		CAM-B3LYP aug-cc-pVTZ		Burcl et al.[24] B97-1/TZ2P	
			HO		VCSF		VCI[3]		VCI[3]		VCI[3]		VCI[3]		VCI[3]	
	cm^{-1}	km/mol														
ν_2	1595	53.6−71.9	49	71.2	−12	71.3520	−19	71.6	−5	73.0	−43	76.6	−49	82.0	−3	74.0
$2\nu_2$	3152	0.461	135		−0	0.4394	−32	0.429	−4	0.452	−91	0.340	−105	0.342	4	0.769
ν_1	3657	2.24−2.98	174	3.13	36	1.9217	39	1.90	84	2.83	12	3.59	57	6.11	9	2.95
ν_3	3756	41.7−44.6	180	54.4	141	51.9388	23	47.9	65	53.3	−5	58.3	40	71.5	9	40.7
$3\nu_2$	4667	0.00238*	263		58	0.0002	−51	0.0021	−10	0.0018	−167	0.0002	−197	0.0000		
$\nu_1+\nu_2$	5235	0.223	240				−9	0.110	51	0.101	−59	0.0774	−18	0.0662	−21	0.205
$\nu_2+\nu_3$	5331	4.50	248				−49	3.84	8	3.88	−99	3.93	−59	4.16	−28	4.14
$4\nu_2$	6134	0.0001*	439		146		−108	0.0003	−56	0.0003	−403	0.0003	−553	0.0003		
$2\nu_1$	7202	0.32	461		211	0.404	158	0.465	249	0.422	114	0.308	203	0.312	28	0.383
$\nu_1+\nu_3$	7250	4.85	518				182	3.19	259	2.95	139	2.65	227	2.55	57	2.45
$2\nu_3$	7468	0.032	404		475	0.508	85	0.0011	147	0.0000	11	0.0003	99	0.0003	23	0.0095

[a] For each calculation, the first column shows the difference between the calculated and experimental line positions (cm^{-1}). The second column shows the calculated intensity (m/mol). For the VCI calculations the 10 lowest VSCF modals have been used. Fundamental modes: ν_1 (A_1), symmetric stretch; ν_2 (A_1), bending; ν_3 (B_2), antisymmetric stretch. [b] As compiled in ref 24 or if marked with *, ref 58.

TABLE 2: Raman Activities (Left Columns, Å/amu) and Depolarization Ratios (Right Columns) Calculated for Water[a]

	Exp.[b]		CCSD d-aug-cc-pVTZ						CCSD/CCSD (T) d-aug-cc-pVTZ VCI[3]		B3LYP aug-cc-pVTZ VCI[3]		CAM-B3LYP aug-cc-pVTZ VCI[3]		CCSD (static) d-aug-cc-pVTZ VCI[3]	
			HO		VSCF		VCI[3]									
	$Å^4$/amu															
ν_2	0.9 ± 0.2	0.726	0.792	0.696	0.995	0.715	0.973	0.713	0.977	0.715	1.26	0.748	1.13	0.749	1.03	0.732
$2\nu_2$					0.0737	0.600	0.0813	0.640	0.0739	0.696	0.0740	0.460	0.0701	0.507	0.0789	0.629
ν_1	111 ± 12	0.0342	119	0.041	129	0.044	129	0.044	129	0.044	109	0.061	117	0.057	115	0.048
ν_3	19 ± 2		27.7	0.750	29.7	0.750	30.5	0.750	30.6	0.750	28.8	0.750	31.0	0.750	27.1	0.750
$3\nu_2$					0.00620	0.308	0.00381	0.667	0.00381	0.592	0.00202	0.747	0.00188	0.750	0.00362	0.635
$\nu_1+\nu_2$							0.404	0.608	0.415	0.597	0.383	0.651	0.372	0.675	0.383	0.629
$\nu_2+\nu_3$							0.00001	0.595	0.00011	0.690	0.00009	0.750	0.00052	0.750	0.00030	0.747
$4\nu_2$					0.00017	0.056	0.00053	0.396	0.00053	0.425	0.00022	0.647	0.00013	0.585	0.00047	0.400
$2\nu_1$					0.0910	0.646	0.159	0.278	0.162	0.276	0.118	0.403	0.120	0.421	0.169	0.186
$\nu_1+\nu_3$							0.00398	0.750	0.00385	0.750	0.00685	0.750	0.00492	0.750	0.00008	0.750
$2\nu_3$					0.268	0.009	0.223	0.011	0.226	0.010	0.121	0.023	0.15	0.015	0.228	0.012

[a] The CCSD/CCSD(T) column is calculated using the CCSD(T) potential but only the CCSD polarizabilities. The excitation wavelength used is 514.5 nm except in the rightmost column where the static polarizabilities from a CCSD/d-aug-cc-pVTZ calculation have been used. [b] From refs 59 and 60.

should be intuitively clear. By truncating the sum in eq 15 at a given excitation level *n*, meaning that only excitations including *n* or less modes are allowed, we obtain VCI[*n*].

Having obtained the vibrational wave functions, the remaining task is to calculate the transition matrix elements, $\langle v_f|\boldsymbol{\mu}(\mathbf{Q})|v_i\rangle$ and $\langle v_f|\alpha_{\rho\sigma}(\mathbf{Q})|v_i\rangle$, e.g., eqs 1 and 10. This is done using response theory as described in, e.g., refs 46−50. The basic idea in response theory is to expand expectation values as well as the parameters of the ground state wave function in orders of a perturbation strength parameter. Using time-dependent variational theory, equations for the response functions, i.e., the coefficients in the expansion of the expectation value, are obtained. In the present case, only the linear response function is needed. The linear response function has poles at the vibrational excitation energies and the residues correspond to the transition matrix elements. The poles and residues can be found by solving an eigenvalue problem. For the VCI case, this eigenvalue problem turns out to be equivalent to solving the standard VCI equations. Thus the calculated energies and transition matrix elements are identical to what would be obtained using the solutions of standard VCI. For VSCF, however, this procedure is not identical to using state specific VSCF to get excited states. Using state specific VSCF the excited states obtained are not orthogonal to the VSCF ground state and one has to take into account the overlap of the states when calculating transition matrix elements. This is avoided using response theory. It should be noted that VSCF response theory does not allow transitions to states with excitations in more than one mode at a time. This is a consequence of the basic VSCF parametrization, which includes only a sum of one-mode variations but no variations in several modes simultaneously.[46]

The question of which Hamiltonian to use is important. In this paper a sum over products form,

$$H = \sum_{t=1}^{N_t} c_t \prod_{m=1}^{M} h_{m,t} \tag{16}$$

is used, where *M* is the number of modes. The kinetic energy operator is represented simply by the second derivatives of the normal coordinates. The effect of this approximation compared to using the full Watson Hamiltonian[51] is examined by example calculations on water in ref 16. Here the effect is seen to be on the order of 10−20 cm^{-1} for the fundamental modes. An important task in the future development of the methods used in the present work is therefore to include the full Watson Hamiltonian. Reference 13 describes a hierarchical way of constructing Taylor expansions of potential energy and property surfaces allowing control over the degree of mode coupling. The expansion of the potential can be characterized by the convention *n*M*m*T, specifying an *m*-order Taylor expansion coupling a maximum of *n* modes. Convergence with respect to the maximum number of coupled modes will be studied using formaldehyde as an example.

Concerning the computational effort spent in calculations of this type, two issues need to be considered. The first is the generation of the potential and property surfaces. For these, a large number of electronic structure calculations are required.

As an example, the 4M4T potential for formaldehyde requires 605 separate electronic energy calculations when no symmetry is used. A somewhat larger molecule with 24 modes requires 3409 calculations for a 2M4T surface, 19 601 for a 3M4T surface, and 189 617 for a full 4M4T surface. Thus, the generation of potential and property surfaces is clearly a very time-consuming part of carrying out explicit anharmonic calculations, especially when high accuracy methods such as CCSD(T) are used. Also, the cost compared to using the double harmonic approximation where only harmonic force constants and gradients of the property surfaces are needed is obviously very large.

Carrying out the actual VCI calculations is a matter of diagonalizing matrices. One problem in this context is the large number of states encountered at high energies. For the water and formaldehyde molecules discussed in this work, however, the VCI solution of relatively low lying states does not pose a problem and is relatively inexpensive.

III. Computational Details

The vibrational calculations have all been carried out using the MidasCpp program.[52] The one-mode basis sets in the VSCF calculations are the harmonic oscillator functions with frequencies corresponding to the normal frequencies of the individual modes. For both water and formaldehyde, functions with quantum numbers up to and including 20 have been used. It has been checked that increasing the number of levels leaves the VSCF energies virtually unchanged. In the VCI calculations it was decided to use the 10 lowest VSCF modals for water and the 8 lowest modals for formaldehyde based on the convergence of calculations with different numbers of modals. The maximum excitation level used for water is 3, corresponding to full VCI. For formaldehyde we decided upon the excitation level 4 as a good compromise between accuracy and the size of the excitation space; see the discussion in section IV B.

The generation of potentials and property surfaces has also been implemented in MidasCpp[52] using DALTON[53] with the DFT[54] and CC[55] electronic response theory implementations for the calculation of the electronic dynamical dipole polarizabilities. In section IV we present results obtained using different electronic structure methods for the generation of these surfaces. Specifically, we have used CCSD(T), CCSD, DFT/B3LYP, and DFT/CAM-B3LYP. For the coupled cluster calculations on water, the d-aug-cc-pVTZ[1,56] basis set has been used. For all other calculations on water and formaldehyde the smaller aug-cc-pVTZ[1,56] basis has been used. Unless otherwise stated, full quartic (4M4T) expansions for energies and properties have been used.

IV. Results

In the following, two different issues are addressed. First, the accuracies of VCI and VSCF are compared to each other as well as to the double harmonic approximation. In addition, the convergence properties with respect to excitation level in VCI are studied. Second, the performance of the DFT functionals B3LYP and CAM-B3LYP in the electronic structure part of the calculations has been studied by comparison with results obtained using CCSD(T) calculations. The molecules studied are water and formaldehyde.

A note should be added about the specification of vibrational states. VCI states are in principle linear combinations of Hartree products of one-mode functions for all levels for all modes. In this paper the convention is to label the states according to the Hartree product with the largest contribution. Thus, the numbering is relative to the VSCF ground state modals, which are anharmonic one-mode levels but, to a certain extent, can be assumed to be in one-to-one correspondence with the harmonic oscillator levels. This is sensible as most of the states, with important exceptions discussed later, only have minor contributions in addition to a dominating Hartree product with weight larger than 90%.

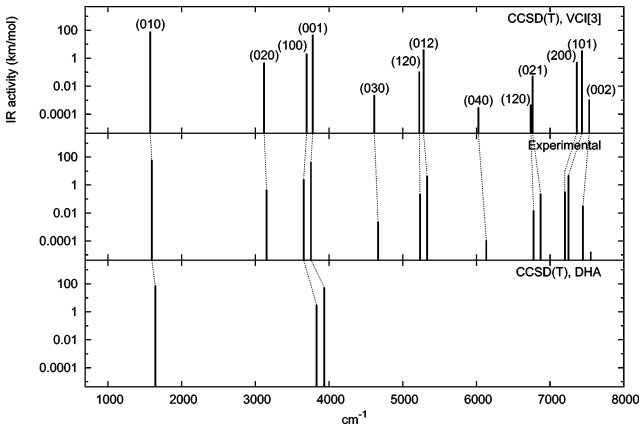

Figure 1. Comparison of experimental, VCI and double harmonic approximation (DHA) line positions and IR intensities for water. The labeling of transitions are ($\upsilon_{\nu_1}\upsilon_{\nu_2}\upsilon_{\nu_3}$). Except for the fourth overtone, $5\nu_5$, with an experimental position of 7552 cm^{-1} and a VCI[3] position of 7265 cm^{-1} all states from 0 to 8000 cm^{-1} are included. Experimental values not included in Table 1 are from ref 58. For transitions with a range of experimental intensities, the average is used in the figure.

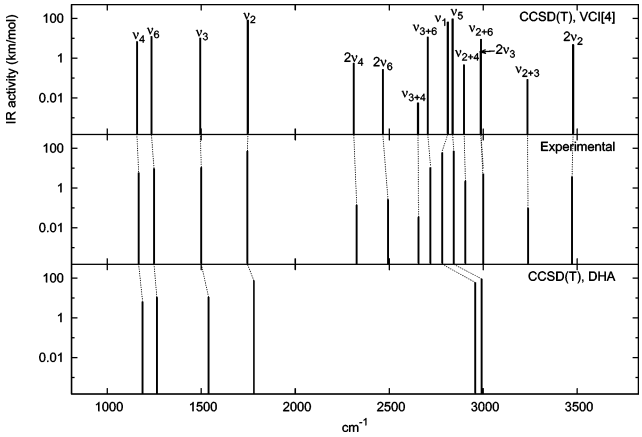

Figure 2. Comparison of experimental, VCI, and double harmonic approximation (DHA) line positions and IR intensities for formaldehyde. All states from 0 to 3500 cm^{-1} are included. For transitions with a range of experimental intensities, the average is used in the figure.

A. Water. Table 1 shows a selection of the calculated energies and IR intensities. Focusing first on the energies from the CCSD(T) calculations, a significant improvement is observed going from the simple harmonic approximation to the VSCF method. Note that the VSCF response theory does not allow calculation of combination bands relative to the reference state. Moving on to the VCI calculation, the magnitude of the errors decreases further. In addition, intensities for all transitions, i.e., overtones and combination bands, are now obtained. The gain obtained using VCI is also very apparent in Figure 1, which shows stick diagrams comparing the experimental line positions and IR intensities to those calculated using CCSD(T) in combination with the double harmonic approximation and VCI-[4], respectively. It should be noted, however, that the figure corresponds to zero temperature. Because the intensities of some overtones and combination bands are very small, the hot bands

TABLE 3: Convergence of VCI in Formaldehyde Calculations[a]

	VCI[2]	VCI[3]	VCI[4]	VCI[5]	VCI[6]	exp[b]
ν_4	15.940	1.244	0.383	0.002	1176.960	1167
ν_6	18.109	0.659	0.010	0.000	1251.202	1249
ν_3	17.558	0.846	0.085	0.001	1514.859	1500
ν_2	16.404	0.802	0.275	0.001	1801.437	1746
$2\nu_4$	16.976	1.511	0.476	0.004	2347.163	2327
$\nu_4+\nu_6$	41.716	19.139	1.120	0.009	2435.540	
$2\nu_6$	25.985	2.600	0.037	0.000	2497.743	2493*
$\nu_3+\nu_4$	36.086	18.868	1.305	0.109	2690.446	2656
$\nu_3+\nu_6$	29.052	12.665	0.292	0.002	2738.687	2719
ν_1	3.101	0.800	0.018	0.000	2841.802	2782
ν_5	10.280	5.895	0.019	0.000	2871.441	2843
$\nu_2+\nu_4$	30.933	17.543	1.246	0.332	2970.080	2905
$2\nu_3$	23.957	2.336	0.144	0.002	3026.402	3000
$\nu_2+\nu_6$	31.789	18.039	0.757	0.004	3054.148	3000
$\nu_2+\nu_3$	24.152	19.259	0.838	0.007	3308.708	3238
$3\nu_4$	20.082	2.165	0.779	0.011	3502.102	
$2\nu_2$	19.847	1.198	0.312	0.003	3586.638	3472

[a] The VCI[2] − VCI[5] energies are relative to the VCI[6] energies. Eight VSCF modals have been used for each mode. The potential used is 4M4T generated using CCSD/aug-cc-pVTZ. All energies are in cm^{-1}. [b] Experimental values from ref 61 or if marked with *, ref 62.

TABLE 4: Convergence of VCI Energies with Respect to Mode Coupling in the Potential Surface[a]

pot.	1M4T 25 points	2M4T 205 points	3M4T 365 points	4M4T 605 points
ν_4	52.7	0.3	0.1	1177.0
ν_6	40.8	3.4	−0.4	1251.2
ν_3	42.6	2.8	−0.4	1514.9
ν_2	14.5	1.1	−0.3	1801.4
$2\nu_4$	128.1	1.2	0.3	2347.2
$\nu_4+\nu_6$	86.2	4.2	0.0	2435.5
$2\nu_6$	97.6	8.9	0.5	2497.7
$\nu_3+\nu_4$	96.7	3.6	−0.1	2690.4
$\nu_3+\nu_6$	110.8	39.6	−18.6	2738.7
ν_1	88.5	0.3	−0.4	2841.8
ν_5	226.8	−17.8	12.5	2871.4
$\nu_2+\nu_4$	75.5	2.1	−0.0	2970.1
$2\nu_3$	88.1	5.7	−1.1	3026.4
$\nu_2+\nu_6$	53.8	−1.5	5.3	3054.1
$\nu_2+\nu_3$	64.7	3.9	−0.7	3308.7
$3\nu_4$	234.2	3.0	0.6	3502.1
$2\nu_2$	31.9	3.0	−0.6	3586.6

[a] The 1M4T, 2M4T, and 3M4T columns are energies (cm^{-1}) relative to the 4M4T energy. "Points" is the number of electronic calculations needed to create the surface not taking into account symmetry. All electronic calculations are CCSD/aug-cc-pVTZ and the vibrational are VCI[6].

appearing at higher temperatures can be expected to alter the appearance of the spectrum significantly.

The experimental IR intensities are not as accurately determined as the energies, thus complicating the comparison with calculated values. However, looking at Figure 1, the CCSD(T) method reproduces the structure of the experimental spectrum very well. Also, from Table 1, satisfactory agreement is observed, although some variations are seen. In particular, for the ν_1 IR intensity both VSCF and VCI[3] are on the low side of experiment whereas the double harmonic approximation is on the high side.

Observing the CCSD results, some transition energies are closer to experiment than the CCSD(T) ones. However, this must be attributed to cancellation of errors. It is noteworthy that the ν_1 intensity is also very sensitive toward this variation in the calculation.

Finally, the DFT calculations are not too far from the CCSD(T) results for the energies of the fundamental vibrations but become progressively worse for the higher excited levels. This may indicate that the range over which the potential can be accurately calculated is not as large as in the CC methods. The intensities are quite far from the CCSD(T) results.

TABLE 5: Convergence of IR Intensities with Respect to Mode Coupling in the Potential and Dipole Surfaces[a]

pot.	1M4T 25 points	2M4T 205 points	3M4T 365 points	4M4T 605 points
ν_4	7.18451	7.19038	7.18652	7.18758
ν_6	10.80461	11.15273	11.48591	11.35579
ν_3	11.21075	12.33833	9.25271	9.36337
ν_2	77.98154	81.62009	85.25562	85.10165
$2\nu_4$	2.64920	0.44865	0.44050	0.43801
$\nu_4+\nu_6$	0.00000	0.00000	0.00000	0.00000
$2\nu_6$	0.20306	0.25310	0.21177	0.28389
$\nu_3+\nu_4$	0.00000	0.00414	0.00934	0.00886
$\nu_3+\nu_6$	0.00000	0.90822	18.36495	12.13911
ν_1	62.73709	63.94433	63.49304	63.00267
ν_5	84.69957	100.21262	75.04414	84.07637
$\nu_2+\nu_4$	0.00000	0.45681	0.46477	0.46445
$2\nu_3$	0.56281	1.70721	1.79480	2.14219
$\nu_2+\nu_6$	0.00000	0.00004	7.37503	4.5421
$\nu_2+\nu_3$	0.00000	0.00053	0.09302	0.12141
$3\nu_4$	0.00005	0.00013	0.00018	0.00018
$2\nu_2$	3.31524	4.29536	4.24203	4.29189

[a] All electronic calculations are CCSD/aug-cc-pVTZ and the vibrational are VCI[6]. Intensities are in km/mol.

Results from a previous study by Burcl et al.[24] are included in the rightmost column. In that study a quartic potential energy surface and cubic dipole moment surfaces were generated using the B97-1 exchange−correlation functional and the TZ2P basis set. Using the MULTIMODE code,[16] VCI[3] was carried out using a basis with 7 modals per mode. In addition, the sum of all vibrational quantum numbers were restricted to 6. Generally, their B97-1 energies are closer to the experimental ones than our B3LYP and CAM-B3LYP results. Concerning the IR intensities, however, we are on par with their results.

Table 2 contains the calculated Raman activities and depolarization ratios. The excitation wavelength used is 514.5 nm. The dynamic polarizabilities cannot be calculated using the CCSD(T) method. For this reason CCSD is used as the primary method. A calculation using the CCSD(T) potential combined with CCSD properties has, however, been included. For the fundamental transitions, there are only small changes between the VSCF and VCI calculations whereas the double harmonic approximation differs by 5−20% from these (all using the CCSD method). For the weak combination bands and overtones, quite large differences are seen in going from VSCF to VCI. The DFT calculations show the same trend as for the IR calculations, i.e., quite large discrepancies between DFT and CC methods. The rightmost column of Table 2 shows the Raman activities obtained using the, in terms of CPU time, slightly less expensive static polarizabilities of a CCSD calculation. Except for the very weak $\nu_2+\nu_3$ and $\nu_1+\nu_3$ bands good agreement is observed with the results obtained from the dynamic polarizabilities.

There is a lack of experimental Raman data for water in the gas phase, and only the activities for the three fundamentals are available for comparison. However, our results show good agreement with these, especially considering that the experimental data are obtained primarily by using the ratios of the activities. Observing the relative activities we obtain

$$\nu_2^{\mathrm{exp}}/\nu_1^{\mathrm{exp}} = 0.0080 \qquad \nu_3^{\mathrm{exp}}/\nu_1^{\mathrm{exp}} = 0.17 \tag{17}$$

For the CCSD/VCI[3] result we obtain

$$\nu_2/\nu_1 = 0.0076 \qquad \nu_3/\nu_1 = 0.24 \tag{18}$$

TABLE 6: Comparison with Experimental IR Line Positions and Intensities for Formaldehyde[a]

	Exp[b]		CCSD(T)						CCSD		B3LYP		CAM-B3LYP		Burckl et al.[24]	
	cm^{-1}	km/mol	HO		VCSF		VCI[4]		VCI[4]		VCI[4]		VCI[4]		B97-1/VCI[4]	
ν_4	1167	5.2−6.5	21	6.58	1	6.36	−9	6.43	10	7.19	−5	5.55	10	6.13	11	4.79
ν_6	1249	9.4−9.9	15	11.1	−4	11.5	−14	11.7	2	11.4	−15	12.4	−3	13.3	−6	9.66
ν_3	1500	11.2	39	11.4	1	10.1	−5	9.81	15	9.39	−9	10.4	−0	1.1	−1	8.60
ν_2	1746	74	34	74.6	6	77.7	2	77.9	56	85.1	40	120	76	124	51	107.2
$2\nu_4$	2327	0.14	50		17	0.471	−16	0.538	21	0.437	−7	0.184	23	0.179	15	0.0238
$\nu_4+\nu_6$	dip. forb.		(2452)				(2404)		(2437)		(2398)		(2425)			
$2\nu_6$	2493[c]	0.27	34		3	0.268	−27	0.260	5	0.284	−29	0.583	−6	0.479	−13	0.832
$\nu_3+\nu_4$	2656	0.036	72				−3	0.0054	36	0.0086	−4	0.0205	20	0.0265	20	0.0359
$\nu_3+\nu_6$	2719	8−14	84				−14	11.0	20	12.2	−33	36.4	−6	19.5	−38	62.8
ν_1	2782	48−75.5	176	59.7	30	62.7	30	62.5	60	63.0	−39	75.6	7	66.9	−48	61.7
ν_5	2843	59−88	148	91.9	86	101	−6	89.0	28	84.1	−48	97.0	−2	91.2	−14	59.2
$\nu_2+\nu_4$	2905	2.3	63				−7	0.439	66	0.465	36	0.482	88	0.451	65	0.505
$2\nu_3$	3000	2.2−2.5	78		8	1.62	−14	2.07	27	2.14	20	2.05	−1	2.38	2	1.33
$\nu_2+\nu_6$	3000	0.5−10	43				−12	8.49	55	4.52	19	3.48	67	2.84	42	4.97
$\nu_2+\nu_3$	3238		81				−3	0.0795	72	0.121	32	0.173	78	0.206	59	0.0861
$3\nu_4$			(3565)		(3561)	0.0003	(3451)	0.0002	(3503)	0.0002	(3467)	0.0001	(3512)	0.0001		
$2\nu_2$	3472	3.8	87		21	4.46	6	4.57	115	4.29	83	4.31	156	4.15	104	3.87

[a] For each calculation, the first column shows the difference between the calculated and experimental energies when experimental energies are available (cm^{-1}). The second column is the calculated IR Intensities (km/mol). All electronic calculations were done using the aug-cc-pVTZ basis. Fundamental modes: ν_1 (A_1), CH symmetric stretch; ν_2 (A_1), CO stretch; ν_3 (A_1), HCH bend; ν_4 (B_1), out-of-plane bend; ν_5 (B_2), CH antisymmetric stretch and ν_6 (B_2), CH_2 rock. [b] Energies from ref 61. Intensities as compiled in ref 24. [c] Reference 62.

TABLE 7: Raman Activities (Å^4/amu, Left Columns) and Depolarization Ratios (Right Columns) Calculated for Formaldehyde[a]

	CCSD						CCSD/CCSD(T)		B3LYP		CAM-B3LYP		CCSD	
	HO		VSCF		VCI[4]		VCI[4]		VCI[4]		VCI[4]		static	
ν_4	0.113	0.750	0.291	0.750	0.266	0.750	0.269	0.750	0.492	0.750	0.340	0.750	0.239	0.750
ν_6	1.06	0.750	1.49	0.750	1.37	0.750	1.41	0.750	1.54	0.750	1.19	0.750	1.28	0.750
ν_3	11.2	0.361	12.1	0.404	11.8	0.402	11.7	0.403	10.9	0.439	10.2	0.427	10.6	0.406
ν_2	11.7	0.213	11.4	0.261	11.6	0.266	11.7	0.269	11.0	0.457	11.3	0.394	9.6	0.225
$2\nu_4$			0.558	0.393	0.573	0.387	0.564	0.381	0.885	0.380	0.830	0.393	0.648	0.361
$\nu_4+\nu_6$					0.0377	0.750	0.0378	0.750	0.0409	0.750	0.0419	0.750	0.0278	0.750
$2\nu_6$			0.726	0.178	0.706	0.166	0.680	0.171	1.31	0.178	1.14	0.166	0.619	0.150
$\nu_3+\nu_4$					0.0309	0.748	0.0323	0.744	0.0367	0.750	0.0387	0.750	0.0297	0.749
$\nu_3+\nu_6$					18.7	0.750	16.2	0.750	46.5	0.750	27.6	0.750	15.2	0.750
ν_1	192	0.099	222	0.101	221	0.101	221	0.101	263	0.114	241	0.110	182	0.094
ν_5	106	0.750	115	0.750	93.3	0.750	92.3	0.749	101	0.750	99.4	0.750	74.1	0.750
$\nu_2+\nu_4$					0.114	0.750	0.116	0.749	0.149	0.750	0.141	0.750	0.0900	0.750
$2\nu_3$			3.58	0.083	4.65	0.085	4.43	0.085	4.61	0.095	5.62	0.092	3.70	0.078
$\nu_2+\nu_6$					6.73	0.750	10.6	0.750	5.41	0.750	4.64	0.750	5.25	0.750
$\nu_2+\nu_3$					1.17	0.054	1.29	0.053	1.23	0.055	1.17	0.055	0.985	0.049
$3\nu_4$			0.0105	0.750	0.00480	0.750	0.00446	0.750	0.0115	0.750	0.0111	0.750	0.00373	0.750
$2\nu_2$			0.704	0.161	0.680	0.166	0.750	0.167	0.971	0.162	0.854	0.151	0.467	0.178

[a] All electronic calculations are done using the aug-cc-pVTZ basis. The CCSD/CCSD(T) column is calculated using the CCSD(T) potential but only the CCSD polarizabilities. The excitation wavelength used is 488 nm except in the last column where static polarizabilities are used.

Thus, the ν_2/ν_1 ratio is in very good agreement with experiment whereas the ν_3/ν_1 value is larger than the experimental value. The same trend was observed in works using the double harmonic approximation by Vidal et al.[27] and Neugebauer et al.[26] In addition to the errors in the electronic and vibrational calculations affecting both the IR and Raman results, it should be noted that the Placzek approximation might also affect the accuracy of the Raman results.

B. Formaldehyde. Formaldehyde has six vibrational degrees of freedom compared to only three for water. For molecules of this size, full VCI is possible in a modest sized modal basis but begins to be impractical because of the heavy scaling with respect to the maximum number of simultaneously excited modes. This problem becomes more pronounced as one proceeds to even larger molecules. For this reason it is interesting to study the convergence properties with respect to excitation level.

Table 3 shows the convergence of the energy with respect to the VCI levels using a 4M4T potential. A significant difference between VCI[2] and VCI[3] is observed. Going from VCI[3] to VCI[4], 7 of the 17 considered states show a change in energy in the interval 5−20 cm^{-1}, indicating that quadruply excited states have a significant weight for these states. The change in going to VCI[5] and VCI[6] is minor, i.e., less than 1.2 cm^{-1}. The same pattern is seen for IR intensities and Raman activities.

The degree of mode coupling in the expansion of the potential has a significant impact on the number of required electronic structure calculations. Table 4 shows the convergence of the energy for different mode couplings along with the required number of electronic structure calculations. Table 5 contains the corresponding IR intensities. Not surprisingly, a large difference is observed in going from 1M4T to 2M4T. Going from 2M4T to 3M4T and 4M4T, most of the energies are relatively stable. In the light of Table 5, the most interesting exceptions to this are the three states $\nu_3+\nu_6$, ν_5 and $\nu_2+\nu_6$, because the IR intensities of these show significant changes. Looking at the VCI results in detail explains this. For the 2M4T case, the actual states are described almost solely (coefficients 0.99, 0.98, and 0.99) by the VSCF reference states. Going to 3M4T, mixing of the states is introduced, the four most important contributions to each state being

$$\nu_3 + \nu_6 \rightarrow 0.84(\nu_3 + \nu_6) - 0.51\nu_5 - 0.10(\nu_2 + \nu_6) + 0.077(\nu_1 + \nu_5) \quad (19)$$

$$\nu_5 \rightarrow 0.80\nu_5 + 0.52(\nu_3 + \nu_6) + 0.25(\nu_2 + \nu_6) - 0.13(\nu_1 + \nu_5) \quad (20)$$

$$\nu_2 + \nu_6 \rightarrow 0.96(\nu_2 + \nu_6) - 0.27\nu_5 + 0.051(\nu_2 + \nu_3 + \nu_6) - 0.049(\nu_3 + \nu_6) \quad (21)$$

Thus the ν_5 state, which has a strong IR transition strength, also contributes to the $\nu_3 + \nu_6$ and $\nu_2 + \nu_6$ states as a result of a coupling introduced by the more accurate 3M4T potential. For example, $\nu_2 + \nu_6$ goes from a value of 4×10^{-5} km/mol for 2M4T to a value of 7.78 km/mol for 3M4T in reasonable agreement with experiment; see Table 6. During the final step to 4M4T, further changes are observed. The Raman activities show a similar behavior.

From the studies of convergence, it was decided to do all vibrational calculations on formaldehyde using VCI[4] with a 4M4T potential.

Table 6 contains the calculated energies and IR intensities obtained using different electronic and vibrational structure methods along with experimental data. Burcl et al.[24] have performed similar studies, i.e., VCI[4] using a fourth-order Taylor expansion of the potential but a third-order expansion of the dipole moment. The electronic structure method was DFT/B97-1 with the TZ2P basis set. These results are also included for comparison.

The CCSD(T)/VCI[4] calculation shows quite good agreement with experiment. This is also evident from Figure 2, which compares the experimental line positions and intensities with the ones calculated using the double harmonic approximation and VCI[4] both with CCSD(T) as the electronic method. As for water, the energies for the fundamentals are significantly improved by VCI and VSCF compared to the double harmonic approximation whereas the IR intensities are quite stable. The structure of the experimental spectrum in Figure 2, including overtone and combination bands, is thus reproduced very well by VCI and in fact better than for water.

CCSD, B3LYP, and CAM-B3LYP also perform well. Comparing with the B97-1 results of Burcl et al., reasonable agreement is also observed. One thing to notice, however, is the intensities of the mixed pair $\nu_3 + \nu_6$ and ν_5. The experimental intensity is about 6 times higher for ν_5 than for $\nu_3 + \nu_6$, which is reproduced by us but not by Burcl et al.[24]

A set of calculations of Raman activities has been performed as well. The results for an excitation wavelength of 488 nm are displayed in Table 7. As previously observed, relatively large changes are seen between the conventional double harmonic approximation and the VSCF method. The most notable difference obtained by using VCI compared to VSCF is the change in the ν_5 activity. This is related to the mixing of states discussed above, eq 20. If one uses the CCSD(T) potential energy surface instead of the CCSD surface in combination with the CCSD polarizabilities, only small changes are observed for all but the $\nu_2 + \nu_6$ and $\nu_3 + \nu_6$ states. Again, this is an indication that subtle changes in the potential can significantly affect the mixing of the components making up the eigenstates.

Concerning the DFT result we find that they agree fairly well among each other and compares much better to the CC results than was the case in the water calculations. A conspicuous feature is that the state $\nu_3 + \nu_6$ seems to be described better by CAM-B3LYP than by B3LYP.

As in the case of water, a CCSD calculation has been carried out using the static polarizabilities. There is a qualitatively good agreement with the dynamical results and, as expected, a trend for the static activities to be somewhat smaller in magnitude.

We have only been able to find relative experimental activities for the formaldehyde fundamentals.[57] The measured ν_1 activity is by far the strongest followed by ν_2 and ν_3 at about one-tenth of this value. The ν_4, ν_5, and ν_6 activities are vanishing. The same trend is observed in our calculations except for the ν_5 mode, which is calculated to be quite strong. This is, however, in good agreement with both the calculated activities accompanying the aforementioned experimental results[57] and also with double harmonic calculations by Neugebauer et al.[26]

V. Summary

We have described how the VSCF and VCI vibrational wave function methods in combination with vibrational response theory can be used for the calculation of the transition matrix elements necessary for describing vibrational IR and Raman spectroscopy.

For the energy and IR intensity calculations reasonable agreement with experiment is observed for the coupled cluster methods. Generally, the results obtained for formaldehyde are better than those for water. This indicates that the potential of the water molecule is more difficult to express using a simple Taylor expansion, this being one of the most significant shortcomings of the present method. In all cases, however, a significant improvement over the standard double harmonic approximation is observed. It is difficult to discuss the quality of the calculated Raman activities due to lack of experimental data.

The vibrational correlation convergence studies on formaldehyde shows that for a molecule of this size, VCI[4] provides sufficient accuracy. Concerning the expansion of the potential, the exclusion of couplings between more than two modes can be a serious problem because quite strong intensities are missed. However, from a practical point of view, it might be necessary to make this sacrifice for large molecules to reduce the number of electronic structure calculations needed.

We have tested the standard B3LYP method and the more recent CAM-B3LYP method for prediction of IR and Raman spectra. Though the methods sometimes give quite different results, there is no clear picture of which is preferable in this context. For water the B3LYP and CAM-B3LYP results were inferior to previous B97-1 results, though better results were obtained for formaldehyde.

The method presented here is limited in scope by the use of Taylor expanded force fields. Grid methods and the inclusion of the full Watson kinetic energy operator are under development, allowing more accurate vibrational response calculations. Furthermore, the use of vibrational response theory in conjunction with vibrational coupled cluster theory is believed to be an alternative, cost-efficient procedure and is presently considered.[30]

References and Notes

(1) Dunning, T. H., Jr. *J. Chem. Phys.* **1989**, *90* (2), 1007−1023.
(2) Papousek, D.; Aliev, M. *Molecular vibrational-rotational spectra, theory and applications of high resolution infrared, microwave and Raman spectroscopy of polyatomic molecules*; Studies in Physical and Theoretical Chemistry 17, 1st ed.; Elsevier Scientific Publishing Co.: Amsterdam, 1982.
(3) Vazquez, J.; Stanton, J. F. *Mol. Phys.* **2006**, *104*, 377−388.
(4) Bowman, J. M. *J. Chem. Phys.* **1978**, *68* (2), 608−610.
(5) Bowman, J. M. *Acc. Chem. Res.* **1986**, *19* (7), 202−208.
(6) Norris, L. S.; Ratner, M. A.; Roitberg, A. E.; Gerber, R. B. *J. Chem. Phys.* **1996**, *105* (24), 11261−11267.

(7) Christiansen, O. *J. Chem. Phys.* **2003**, *119* (12), 5773−5781.
(8) Bowman, J. M. *J. Phys. Chem.* **1979**, *83* (8), 905−912.
(9) Christoffel, K. M.; Bowman, J. M. *Chem. Phys. Lett.* **1982**, 85 (2), 220−224.
(10) Christiansen, O. *J. Chem. Phys.* **2004**, *120* (5), 2149−2159.
(11) Thompson, T. C.; Truhlar, D. G. *Chem. Phys. Lett.* **1980**, *75*, 87.
(12) Christiansen, O. *J. Chem. Phys.* **2004**, *120* (5), 2140−2148.
(13) Kongsted, J.; Christiansen, O. *J. Chem. Phys.* **2006**, *125* (12), 124108.
(14) Barone, V. *J. Chem. Phys.* **2005**, *122*, 014108.
(15) Ingamells, V. E.; Papadopoulos, M. G.; Raptis, S. G. *Chem. Phys. Lett.* **1999**, *307*, 484.
(16) Bowman, J. M.; Carter, S.; Huang, X. *Int. Rev. Phys. Chem.* **2003**, *22* (3), 533−549.
(17) Yagi, K.; Hirao, K.; Taketsugu, T.; Gordon, M. S. *J. Chem. Phys.* **2004**, *121*, 1283.
(18) Hollebeek, T.; Ho, T. S.; Rabitz, H. *Annu. Rev. Phys. Chem.* **1999**, *50*, 537−570.
(19) Zhang, X. B.; Zou, S. L.; Harding, L. B.; Bowman, J. M. *J. Phys. Chem. A* **2004**, *108*, 8980−8986.
(20) Rauhut, G. *J. Chem. Phys.* **2004**, *121*, 9313−9322.
(21) Bishop, D. M.; Kirtman, B. *J. Chem. Phys.* **1991**, *95*, 2646−2658.
(22) Car, R.; Parrinello, M. *Phys. Rev. Lett.* **1985**, *55*, 2471−2474.
(23) Ramirez, R.; López-Ciuda, T.; Kumar, P. P.; Marx, D. *J. Chem. Phys.* **2004**, *121*, 3973−3983.
(24) Burcl, R.; Carter, S.; Handy, N. C. *Chem. Phys. Lett.* **2003**, *380* (3−4), 237−244.
(25) Oyanagi, C.; Yagi, K.; Taketsugu, T.; Hirao, K. *J. Chem. Phys.* **2006**, *124* (6), 064311.
(26) Neugebauer, J.; Reiher, M.; Hess, B. A. *J. Chem. Phys.* **2002**, *117* (19), 8623−8633.
(27) Vidal, L. N.; Vazquez, P. A. M. *Int. J. Quantum Chem.* **2005**, *103* (5), 632−648.
(28) Zalesny, R.; Bartkowiak, W. *Int. J. Quantum Chem.* **2005**, *104* (5), 660−666.
(29) Svendsen, E. N.; Oddershede, J. *J. Chem. Phys.* **1979**, *71* (7), 3000−3005.
(30) Seidler, P.; Christiansen, O. *J. Chem. Phys.*, submitted for publication.
(31) Yanai, T.; Tew, D. P.; Handy, N. C. *Chem. Phys Lett.* **2004**, *393* (1−3), 51−57.
(32) Partridge, H.; Schwenke, D. W. *J. Chem. Phys.* **1997**, *106*, 4618−4639.
(33) Polyansky, O. L.; Csaszar, A. G.; Shirin, S. V.; Zobov, N. F.; Barletta, P.; Tennyson, J.; Schwenke, D. W.; Knowles, P. J. *Science* **2003**, *299*, 539−542.
(34) Bansil, R.; Berger, T.; Toukan, K.; Ricci, M. A.; Chen, S. H. *Chem. Phys. Lett.* **1986**, *132*, 165−172.
(35) Silvestrelli, P. L.; Bernasconi, M.; Parrinello, M. *Chem. Phys. Lett.* **1997**, *277*, 478−482.
(36) Romanowski, H.; Bowman, J. M.; Harding, L. B. *J. Chem. Phys.* **1985**, *82*, 4155.
(37) Martin, J. M. L.; Lee, T. J.; Taylor, P. R. *J. Mol. Spectrosc.* **1993**, *160*, 105−116.
(38) Carter, S.; Pinnavaia, N.; Handy, N. C. *Chem. Phys. Lett.* **1995**, *240*, 400−408.
(39) Burleigh, D. C.; McCoy, A. B.; Sibert, E. L. *J. Chem. Phys.* **1996**, *104*, 480.
(40) Yagi, K.; Oyanagi, C.; Taketsugu, T.; Hirao, K. *J. Chem. Phys.* **2003**, *118*, 1653−1660.
(41) Poulin, N. M.; Bramley, M. J.; Carrington, T.; Kjaergaard, H. G.; Henry, B. R. *J. Chem. Phys.* **1996**, *104*, 7807−7820.
(42) Mortensen, O. S.; Svendsen, E. N. *J. Chem. Phys.* **1980**, *74* (6), 3185.
(43) Craig, D. P.; Thirunamachandran, T. *Molecular Quantum Electrodynamics*; John Wiley & Sons: New York, 1998.
(44) Long, D. A. *The Raman Effect*; John Wiley & Sons: New York, 2002.
(45) Placzek, G. *Z. Phys.* **1931**, *70*, 84.
(46) Christiansen, O. *J. Chem. Phys.* **2005**, *122* (19), 194105.
(47) Sasagane, K.; Aiga, F.; Itoh, R. *J. Chem. Phys.* **1993**, *99* (5), 3738−3778.
(48) Christiansen, O.; Jørgensen, P.; Hättig, C. *Int. J. Quantum Chem.* **1998**, *1* (1), 1−52.
(49) Christiansen, O.; Kongsted, J.; Paterson, M. J.; Luis, J. M. *J. Chem. Phys.* **2006**, *125* (21), 214309.
(50) Olsen, J.; Jørgensen, P. In *Modern Electronic Structure Theory*; Yarkony, D. R., Ed.; World Scientific: Singapore, 1995; Vol. 2, Chapter 13, pp 857−990.
(51) Watson, J. K. G. *Mol. Phys.* **1968**, *15*, 479−490.
(52) Christiansen, O.; Hansen, M. B.; Kongsted, J.; Paterson, M. J.; Seidler, P.; Toffoli, D. MidasCpp (Molecular Interactions, Dynamics and Simulation Chemistry program package in C++). University of Aarhus, 2006.
(53) DALTON, A molecular electronic structure program, Release 2.0 (2005), see http://www.kjemi.uio.no/software/dalton/dalton.html.
(54) Sałek, P.; Vahtras, O.; Helgaker, T.; Ågren, H. *J. Chem. Phys.* **2002**, *117*, 9630−9645.
(55) Christiansen, O.; Halkier, A.; Koch, H.; Jørgensen, P.; Helgaker, T. *J. Chem. Phys.* **1998**, *108*, 2801−2816.
(56) Kendall, R. A.; Dunning, T. H., Jr.; Harrison, R. J. *J. Chem. Phys.* **1992**, *96* (9), 6796−6806.
(57) Wiegeler, W.; Bleckmann, P. *J. Mol. Struct.* **1980**, *66*, 273−280.
(58) Kjaergaard, H. G.; Henry, B. R.; Wei, H.; Lefebvre, S.; Tucker Carrington, J.; Mortensen, O. S.; Sage, M. L. *J. Chem. Phys.* **1994**, *100* (9), 6228−6239.
(59) Murphy, W. F. *Mol. Phys.* **1977**, *33* (6), 1701−1714.
(60) Murphy, W. F. *Mol. Phys.* **1978**, *36* (3), 727−732.
(61) Reisner, D. E.; Field, R. W.; Kinsey, J. L.; Dai, H.-L. *J. Chem. Phys.* **1984**, *80* (12), 5968−5978.
(62) Ito, F.; Nakanaga, T.; Takeo, H. *Spectrochim. Acta. A* **1994**, *50* (8−9), 1397−1412.